Egypt. J. Chem. **Vol. 65,** No. 2 pp. 307 - 313 (2022)

Egyptian Journal of Chemistry

http://ejchem.journals.ekb.eg/

Study of mechanical properties and wear behavior of nano-ZrO_2-hardened Al2024 matrix composites prepared by stir cast method

Rasha A. Youness [1], Mohammed A. Taha [2,*]

[1.] *Spectroscopy Department, National Research Centre, El Buhouth St., 12622 Dokki, Giza, Egypt*
[2.] *Solid State Physics Department, National Research Centre, El Buhouth St., 12622 Dokki, Giza, Egypt;*

Abstract

The Al2024 matrix composites reinforced by different weight percentages of nano-ZrO_2 particles were prepared by stir-cast method. Physical and mechanical properties (microhardness, compressive test and elastic moduli) of the prepared composites samples were measured. Moreover, the effect of sliding distance and applied load on the wear behavior of all prepared samples was studied. The results showed that the relative density of the Al2024 matrix decreased with the increase ZrO_2 nanoparticles content while the apparent porosity increased. Moreover, the microhardness, ultimate strength and Young's modulus of the composites were improved with increasing of ZrO_2 content except fracture strain that reduced significantly. The wear rate decreased as the reinforcement content increased while it increased with the increase of the sliding distance and applied load. The microhardness, ultimate strength, bulk modulus of the composites containing 10 wt.% ZrO_2 sample improved to approximately 31, 60 and 49%, respectively. For the same sample, the wear rate improved around 20.2 and 21.3 under applied loads 10 and 40 N, respectively.

Keywords: Al2024; Al matrix composites; Mechanical properties; Wear behavior; Stir cast method.

Introduction

A composite material is a macroscopic combination of two or more distinct materials that exhibit a significant proportion of properties than those of the individual components used alone [1-5]. Thus, a better combination of characteristics is achieved. Composite materials are of great importance in many fields, whether industrial applications or biomedical applications due to their improved properties, high strength, high stiffness and low density [6-10]. Among composite materials, aluminum (Al) and Al alloy matrix composites enjoy remarkable interest in aerospace, automobile and electronic equipment because of their attractive properties such as high strength, excellent young's modulus, elevated wear resistance, and low thermal expansion coefficient [3, 11-13]. It is well known that by selecting the suitable ceramic reinforcement, better properties of Al matrix composites could be produced. A variety of particulate ceramic reinforcements like Al_2O_3 [14, 15], SiC [16], ZrO_2 [17] and graphene [18] have been used to reinforce the Al and Al alloy matrix. All reports confirmed that these ceramics effectively enhance the mechanical and tribological properties of the final composites. Taha *et al*. [17] milled ZrO_2 nanoparticles with Al alloy powder by mechanical alloying to produce nanocomposite powders contain different contents of ZrO_2. Then, they were pressed and sintered in the argon atmosphere to produce bulk nanocomposite samples. The microhardness and compressive strength of the nanocomposites were significantly increased by increasing the ZrO_2 content. Mungara *et al*. [19] produced Al7050 matrix composites reinforced with various weight percentages of B_4C particles up to 8 wt.% by stir-casting. The resulting composites have uniform distribution of B4C reinforcement in the matrix. Additionally, the linear relation between the mechanical parameter and the B_4C weight percentages is unique. Among these reinforcement, fine stabilized ZrO_2 particles could be a suitable reinforcing material due to their high hardness,

*Corresponding author e-mail: mtahanrc@gmail.com. (M.A. Taha)
Receive Date: 10 July 2021, Revise Date: 29 July 2021, Accept Date: 25 August 2021
DOI: 10.21608/EJCHEM.2021.85000.4154

ultimate strength and stiffness, high melting temperature (2715 °C), high wear rate, and good corrosion resistance [20, 21]. Noteworthy, many techniques have been developed in the recent past for the manufacture of composites. Different processing methods like mechanical alloying [18, 22, 23], spray casting [24], fracture stir [25, 26] and stir-cast [27, 28]. Among the manufacturing techniques, stir-casting is a type of casting process in which a vortex is formed by a mechanical stirrer to mix the reinforcement into an Al matrix. It is a suitable method for preparing Al matrix composites due to its simplicity, low cost, applicability to mass production, simplicity, very low porosity content and ease of control of the composite structure [29, 30]. Based upon the above considerations, the aim of the current work is to study the effect of variable nano-ZrO_2 percentage on the microstructure, physical, mechanical and ware properties of Al2024 alloy prepared by stir cast.

Materials and Methods

Al2024-ZrO_2 composites have been prepared by stir-casting process. The different weight percentages of ZrO_2 particles (0, 2.5, 5, 7.5 and 10 wt. %) were used in this work as a reinforcement from Al Nasr company having a particle size of 50 nm. The Al2024 matrix was melted at 800°C, while the nano- ZrO_2 particles were heated in a furnace at 400 °C for 1 h to remove moisture from the surface of the particles and after that ZrO_2 particles were added slowly in the center of the vortex. The melt was thoroughly stirred for 20 min to obtain a better distribution of the reinforcement particles. Then, the melt was poured into a preheated iron mold. The bulk density of the prepared composites was measured by Archimedes method according to ASTM: B962-08. As described in our recent work [31-33], the microhardness of all investigated samples was measured according to ASTM: B933-09 using 1.96 N loads under dwell time of 10 s according to Eq. (1) [34, 35]:

$$Hv = 1.854 \text{ x } \frac{P}{D^2} \quad \text{…….. (1)}$$

The stress-strain curve was measured and the values of tensile strength, yield strength and ductility were calculated accordingly. Ultrasonic longitudinal and shear wave velocities (i.e. V_L and V_S) were propagated in the sintered nanocomposites specimen, using pulse-echo technique MATEC Model MBS8000 DSP (ultrasonic digital signal processing) system. The values of Lame's constants, *i.e.* λ and μ are obtained from V_L and V_S as follows [36, 37]:

$$\lambda = \rho(V_L^2 - 2V_S^2) \quad \text{…….. (2)}$$

$$\mu = \rho V_S^2 \quad \text{…….. (3)}$$

where ρ is the material bulk density

The values of the elastic moduli; longitudinal modulus (*L*), shear modulus (*G*), Young's modulus (*E*), bulk modulus (*B*) and Poisson's ratio (*v*) as calculated from the following equations [23, 38]:

$$L = \lambda + 2\mu \quad \text{…….. (4)}$$

$$G = \mu \quad \text{…….. (5)}$$

$$E = \mu\frac{3\lambda+2\mu}{\lambda+\mu} \quad \text{…….. (6)}$$

$$B = \lambda + \frac{2}{3}\mu \quad \text{…….. (7)}$$

$$\upsilon = \frac{\lambda}{2(\lambda+\mu)} \quad \text{…….. (8)}$$

The nanocomposite samples were subjected to wear test under dry sliding conditions using at room temperature using a pin-on-disk wear-testing apparatus and the samples of 20 mm in diameter and 7 mm in height. The process parameters of wear test involved speed of 0.8 m/s, sliding distance 200 m and different applied loads of 10, 20 and 40 N. The wear rate (W) was calculated for sintered nanocomposite samples by the following equation [39]:

$$W\ (mm^3/km) = \frac{M}{\rho\ x\ D} \quad \text{…….. (9)}$$

where *M* is the weight loss (g), ρ is the bulk density (g/mm3) and *D* (m) is the sliding distance (m).

Results and Discussion

Physical properties

Fig. 1 displays the influence of nano-ZrO_2 particulates percentages on the relative density and apparent porosity of the composites samples. The theoretical density value for the composites containing 2.5, 5, 7.5 and 10 wt.% ZrO_2 was 2.780, 2.816, 2.853, 2.891 and 2.930 g/cm^3, respectively, while the relative density value for the same samples was 98.39, 97.22, 96.16, 94.23 and 93.11 g/cm^3, respectively. It was observed that the relative density decreases while apparent porosity of the composites increases with the increase in the percentage of ZrO_2 particulates; this is because the variation in the density of the Al alloy matrix and the ZrO_2 reinforcement coupled with an increase in the number of phase boundaries between the Al alloy and ZrO_2 which consequently, causes an increase in the number of pores. Furthermore, the uniform reduction in the relative density and the increase in the apparent

porosity are attributed to the uniform distribution of nano-ZrO_2 in the Al alloy matrix [19, 40]. Another reason is that tensile stresses due to a large difference in the coefficient of thermal expansion (CTE) between the matrix and the reinforcement (CTE of Al alloy and ZrO_2 are $23.2x10^{-6}$ and $10.5x10^{-6}$, respectively), would normally form defects such as porosity and dislocations around the ZrO_2 particles [41]. A Similar interpretation [42] has been reported for the reinforcement of the Al-Si alloy matrix by SiC, which stated that SiC reinforcement directly affected the contacts between it and the Al matrix and therefore, closed pores are formed. After that, the relative density of the composites and the apparent porosity decrease with the increase of the SiC weight percentages.

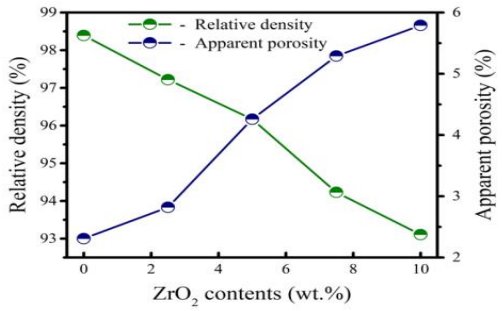

Fig. 1 The relative density and apparent porosity of Al2024-ZrO_2 composites as a function of ZrO_2 contents.

Microstructure

SEM microstructures of as cast Al2024-xZrO_2 (x=0, 5 and 10 wt. %) composites samples are shown in Fig. 2(a-c). Fig 2.a shows that high densification and no porosity appear. The composite contains 5 and 10 wt. % ZrO_2 particles which segregated within the Al2024 matrix and grain boundary during stir cast processing. The microstructure reveals the presence of small amount of porosity associated with the ZrO_2 particles. Moreover, the porosity observed around ZrO_2 particles and subsequence, with increase the ZrO_2 from 5 to 10 wt. %, the amount of porosity in the composite samples increased and indicates weak bonding.

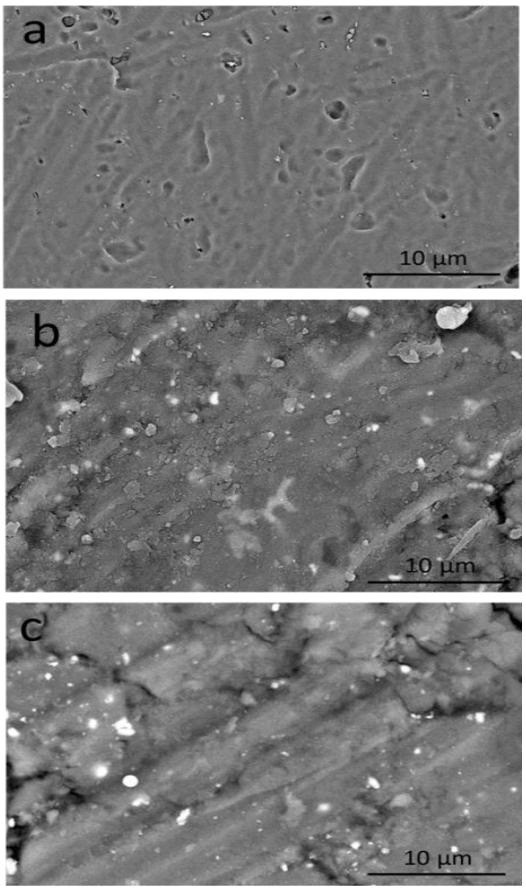

Fig. 2. SEM microphotographs of a) Al2024 alloy, b) Al2024–5 wt. % ZrO_2 and c) Al2024–5 wt.% ZrO_2 composites

Fig. 3 shows the graph of microhardness of Al2024-xZrO_2 (x=0, 2.5, 5, 7.5 and 10 wt.%) composites. The results showed that the microhardness of the composites samples increased with the increases in the weight percentages of ZrO_2. The observed microhardness of pure Al2024 is 36±3 MPa, which reaches a maximum value of 67±4 HV for the composite containing 10 wt.% ZrO_2. Fig. 4 illustrates the effect of ZrO_2 contents on Young's modulus (E), elastic modulus (L), shear modulus (G), bulk modulus (K) and Poisson's ratio (ν) of the composites. It is evident from the figure that the value all elastic moduli increased after reinforced with different weight percentages of nano-ZrO_2 particles. The shear modulus and Poisson's ratio increased to 45.19 GPa and 0.3185 for composites samples containing 10 wt.% ZrO_2 particles.

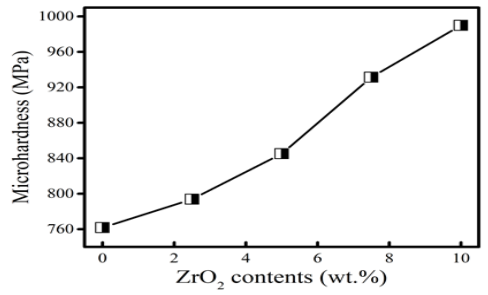

Fig. 3. Microhardness of Al2024-ZrO_2 composites at different ZrO_2 contents.

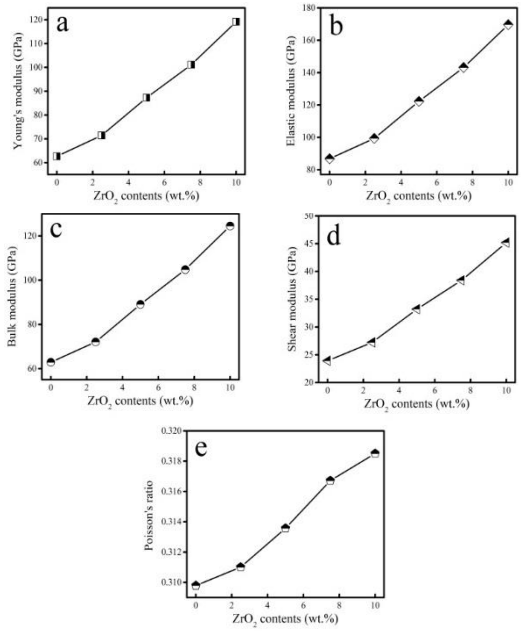

Fig. 4. The effect of ZrO_2 content on the elastic moduli group of Al composites samples.

Fig. 5 shows the representative compressive stress–strain in the room temperature plots of the Al2024/ZrO_2 composite with different reinforcement percentages. The calculated ultimate strength, yield strength and elongation of the Al2024 composites from the corresponding stress–strain curves are shown in Fig. 5. It obvious that from Figs. 6, adding a reinforcement of nano-ZrO_2 particles to the Al2024 matrix increases the ultimate and yield strengths whereas the fracture strain shows the opposite tendency. The ultimate and yield strengths values of the Al2024/ZrO_2 composites were significantly increased from 179.2 and 52.89 MPa to 285.6 and 68.39 MPa, respectively, (the percentages of such increase were 36%, and 63%, respectively) as a result of the incorporation of 10 wt.% of ZrO_2. These results can be discussed by knowing that adding a very hard ceramic (i.e. ZrO_2) phase to a ductile one (i.e. Al 2024 matrix) leads to more dislocation density which gives these composites the appropriate mechanical properties. The presence of nano-ZrO_2 particles can improve the microhardness of composites (H_C) according to Eqn. [43]

$$H_C = H_{Al}F_{Al} + H_ZF_Z \quad \text{..... (10)}$$

where H_{Al} and H_Z represent microhardness of the Al 2024 and the ZrO_2 particle, respectively. However, F_{Al} and F_Z represent the volume fraction of Al2024 and ZrO_2 particles, respectively.

The coefficient of thermal expansion (CTE) of ZrO_2 reinforcement particles is lower than that of Al2024 matrix (CTE of Al2024 and ZrO_2 were 23.2 and 12.2×10^{-6}/K). So, an amount of dislocations are generated at the ZrO_2 particles-Al2024 matrix interface during solidification process, which further increases the mechanical properties of the matrix. The greater the amount of interface between the reinforcement and the matrix, the greater the hardening due to dislocations [44]. On the other hand, the strengthening mechanism resulting from the dispersion of the hardening reinforcement (i.e. ZrO_2) into the matrix (i.e. Al2024) is known as Orowan strengthening. Importantly, the presence of a ZrO_2 reinforcement retards the movement of dislocations in the matrix during the dispersion strengthening mechanism as given by the equation (11)[45]:

$$\sigma_{Orowan} = \frac{0.13Gb}{\lambda} \mathrm{Ln}\frac{r}{b} \quad \text{..... (11)}$$

where, G represents the shear modulus of Al2024 matrix, b represents Burgers vector of Al2024 matrix, r is the radius of nanoparticles and λ represents the inter-particle spacing.

The interparticle spacing is given by the following equation (12)[18]:

$$\lambda = \frac{4(1-f)r}{3f} \quad \text{..... (12)}$$

where f is the ZrO_2 reinforcement volume fraction

According to equation (3), the distance between the particles decreases with the increase in the contents of ZrO_2 thus resulting in an increase in the compressive stress required (T_0) for the movement of dislocations between the ZrO_2 particles leading to an improvement in the composite strength (Eqn.13) [46]:

$$T_0 = \frac{Eb}{\lambda} \quad \text{..... (13)}$$

where E is the elastic modulus of composite and b is the Burger's vector.

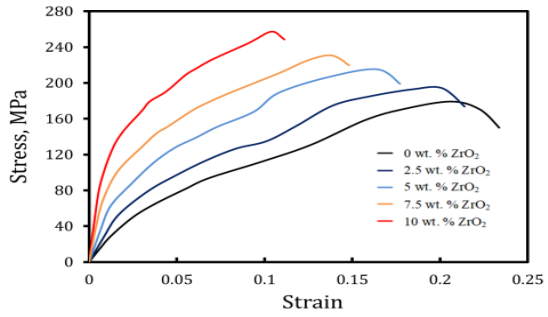

Fig. 5. Tensile stress-strain curve for Al2024-ZrO_2 composites samples.

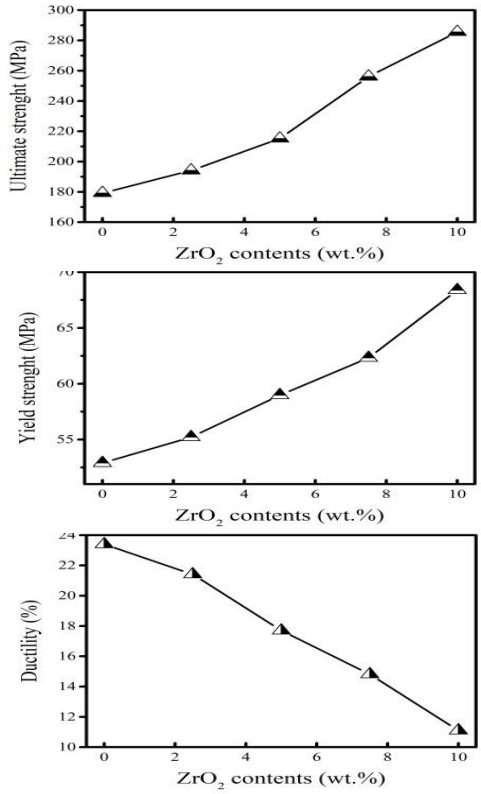

Fig. 6. a) The ultimate strength, b) yield strength and c) elongation of the composites samples.

Fig. 7 shows the strengthening efficiency, R_a, of composites samples as a function of ZrO_2 contents. Noteworthy, R_a can be defined as the ratio of the amount of increase in the yield strength of Al2024-ZrO_2 composite to that of the Al2024 matrix by the addition of ZrO_2 reinforced particles [47]. It is noted from this figure that the improvement of R_a is due to an increase in the weight percentages of ZrO_2 particles. The value of R_a can be calculated by Eqn. 14[3]:

$$R_a = \frac{\sigma_c - \sigma_m}{V\sigma_m} \quad \text{..... (14)}$$

where σ_c is the yield strength of composite, σ_m is the yield strength of the Al2024 matrix, V is volume fraction of ZrO_2 particles.

It is observed that R_a of reinforcement in the Al2024 matrix composites increases in the weight percentages of ZrO_2.

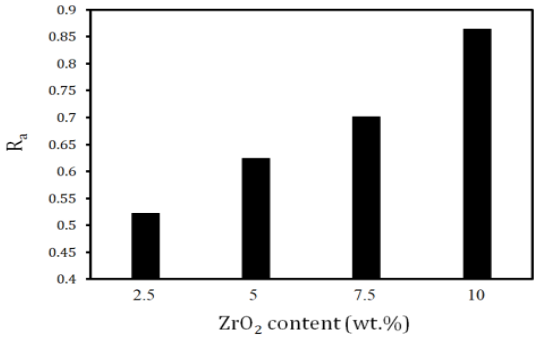

Fig.7. Strengthening efficiency, R_a, for composites at various ZrO_2 contents.

Wear behavior

Figs. (8&9) demonstrate the variation of the wear rate of Al2024-ZrO_2 with a sliding distance under an applied load of 10 and 30 N. As the slip distance increases at the same applied load, there is a higher wear rate for the Al matrix and composites samples. For the Al2024 matrix under 10 N applied load, the wear rate at the sliding distance of 200, 400, 600, 800 and 1000 m was 4.45, 4.84, 5.48, 5.92 and 6.20 mm^3/Km, respectively while the sample had the highest content of ZrO_2 (10 wt.%) and with the same applied load, the wear rate was 3.94, 4.18, 4.37, 4.59 and 4.90 mm^3/Km, respectively. This may be attributed to the increased sliding distance, as the temperature of the sliding surfaces elevated, causing the Al2024 matrix and the composite pin surfaces to soften, resulting in greater deformation at higher sliding distances [48]. It is also evident; the wear rate of the composites samples was significantly lower when compared to the Al alloy matrix and this is due to the enhancement of the microhardness of the composites with an increase in ZrO_2 content. This relationship is more clarified by observing Archard equation [39]:

$$Q = K\frac{W}{H} \quad \text{..... (15)}$$

where Q is wear rate, K is a constant called wear coefficient, W is the applied load and H is the microhardness of the sample.

On the other hand, the wear rate of all samples increased with increasing the applied load from 10 to 40 N. For example, the wear rate of Al2024 and

composites containing 10 wt.% ZrO_2 under the applied load 10 N and the sliding distance 1000 m was 6.20 and 4.90 mm^3/Km, respectively and when the applied load was increased to 40 N at the same sliding distance, the wear rate was 8.24 and 6.55 mm^3/Km, respectively. Generally, an increase in the applied load leads to a plastic deformation on the subsurface due to an increase in the penetration depth of the counterface. Moreover, with an increase in the applied load, the surface temperature increases and consequently encourages surface softening which leads to further surface as well as subsurface deterioration giving increased weight loss [49, 50]

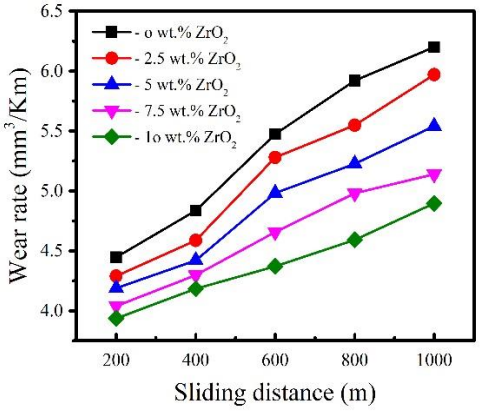

Fig. 8. Wear rate of the composites samples under an applied load of 10 N and the different sliding distance.

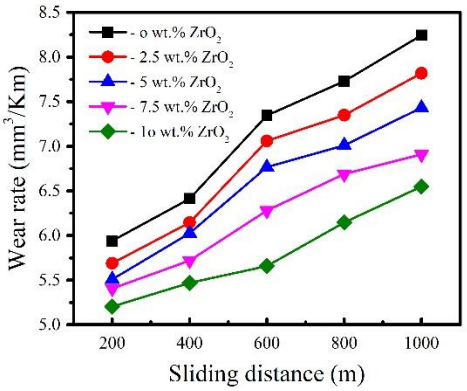

Fig. 9. The wear rate of the composites sample under 40 N applied load and different sliding distance.

Conclusions

- Al2024-ZrO_2 composites with different nano-ZrO_2 contents have been successfully produced by stir-casting method.
- The relative density of composites decreased considerably with an increase in weight percentages of ZrO_2 while, the apparent porosity exhibited an opposite trend.
- The microhardness of the composites increased with the increase in the weight percentages of ZrO_2. The highest Microhardness (990 MPa) was obtained for 10 wt.% of ZrO_2 particles.
- For the compressive test, the ultimate and yield strength of the composites increased while the elongation decreased with the increase in the content of ZrO_2.
- The measured yield strength value of the composite containing 10 wt.% ZrO_2 were 68.4 and 11.1 % MPa, respectively.
- Noticeable enhancement in elastic moduli group with increased ZrO_2 content. For example, the elastic modulus and Poisson's ratio were increased from 86.8 GPa and 0.3098 to 169.7 GPa and 0.3185 with increase in ZrO_2 content from 0 to 10 wt.% , respectively.
- The wear rate decreased with increasing ZrO_2 content while it increased with the sliding distance applied load. The wear rate of Al2024 under the applied load 10 N and the sliding distance 200 and 1000 m was 4.45 and 6.21mm^3/Km, respectively while the wear rate of Al2024-10 wt.% ZrO_2 was 3.937 and 4.9021mm^3/Km, respectively.

References

[1] M.A. Taha, A.H. Nassar, M.F. Zawrah, Constr. Build. Mater. 248 (2020) 118638. 118638.
[2] M.A.Taha, E.B. Moustafa, INT. J. Min. Met. Mater. 28 (2020) 475.
[3] R.A.Youness, M.A. Taha, M.A. Ibrahim, Biointerface. Res. Appl. Chem. 11 (2) (2020) 8946.
[4] R.A.Youness, M.A. Taha, Egypt. J. Chem. 64 (12) (2021) 7215.
[5] W.S. AbuShanab, E.B. Moustafa, M.A. Taha, R.A. Youness, Appl. Phy. A. 126 (10) (2020) 1.
[6] M.A. Taha, R.A. Youness, M. Ibrahim, Ceram. Int. 46 (15) (2020) 23599.
[7] R.A. Youness, M.A. Taha, M.A. Ibrahim, Mater. Chem. Phy. 239 (2020) 122011.
[8] R.A. Youness, M.A. Taha, M. Ibrahim, Mater.Chem. Phys. 257 (2021) 123264.

[9] R.A. Youness, M.A. Taha, A.A. El-Kheshen, M. Ibrahim, Ceram. Int. 44 (17) (2018) 20677.
[10] D.E. Abulyazied, A.M. Alturki, R.A. Youness, H.M. Abomostafa, J. Inorg. Organomet. Polym. Mater 31 (2021) 4077.
[11] W.S. AbuShanab, E.B. Moustafa, E. Ghandourah, M.A. Taha, Silicon (2021) In Press.
[12] B. Xiong, K. Liu, Q. Yan, W. Xiong, X. Wu, Alloy. Compd. 837 (2020).
[13] M.F. Zawrah, W.M. El-Meligy, H.A. Saudi, S. Ramadan 4, M.A. Taha, Biointerface Res. Appl. Chem. 12 (2) (2022) 2068.
[14] M.A. Taha, M.F. Zawrah, Silicon 10 (4) (2017) 1351.
[15] M. Toozandehjani, F. Ostovan, K.R. Jamaludin, A. Amrin, K.A. Matori, E. Shafiei, T. Nonferr. Metal. Soc. 30(9) (2020) 2339.
[16] T. Lu, T. He, Z. Li, H. Chen, X. Han, Z. Fu, W. Chen, Mater. Res. Technol. 9 (6) (2020) 13646.
[17] M.A. Taha, G.M. Elkomy, H.A. Mostafa, E.S. Gouda, Mater. Chem. Phy. 206 (2018) 116.
[18] W.S. AbuShanab, E.B. Moustafa, E. Ghandourah, M.A. Taha, Res. Phy. 19 (2020)103343.
[19] S.R. Mungara, H.S. Manohar, M.A. Trishul, Mater. Today Proceedings 37 (2) (2021) 1463.
[20] M. Elmahdy, G. Abouelmagd, A.A. Mazen, Int. Mater. Res. 108 (12) (2017) 1103.
[21] M.A. Taha, M.F. Zawrah, Ceram. Int. 43 (15) (2017) 12698.
[22] R.A. Youness, M.A. Taha, M. Ibrahim, Ceram. Int. 44 (17) (2018) 21323.
[23] R.A. Youness, M.A. Taha, M.A. Ibrahim, J. Mol. Struct. 1150 (2017) 188.
[24] F.J. Amaya Suazo, S. Shaji, D.A. Avellaneda, J.A. Aguilar-Martínez, B. Krishnan, Solar Energy 207 (2020) 486.
[25] E.B. Moustafa, A. Melaibari, M. Basha, Ceram. Int. 46 (10) (2020) 16938.
[26] W.S. AbuShanab, E.B. Moustafa, Mater. Res. Technol. 9 (4) (2020) 7460.
[27] B. Jayendra, D. Sumanth, G. Dinesh, M.V. Rao, Mater. Today Proceedings 21 (2020) 1104.
[28] S.O. Akinwamide, O.J. Akinribide, P.A. Olubambi, Alloys. Compd. 850 (2021) 126586.
[29] B. Vijaya Ramnath, C. Elanchezhian, M. Jaivignesh, S. Rajesh, C. Parswajinan, A. Siddique Ahmed Ghias, Mater. Des. 58 (2014) 332.
[30] S. Poria, P. Sahoo, G. Sutradhar, Mater. Today Proceedings 5 (11) (2018) 23629.
[31] E.M.A. Khalil, R.A. Youness, M.S. Amer, M.A. Taha, Ceram. Int. 44 (7) (2018) 7867.
[32] R.A. Youness, M.A. Taha, M. Ibrahim, Silicon 10(3) (2017) 1151.
[33] R.M. Khattab, H.E.H. Sadek, M.A. Taha, A.M. El-Rafei, Mater. Charact. 171 (2021) 110740.
[34] H.E.H. Sadek, M.A. Hessien, Z.A. Abd El-Shakour, M.A. Taha, R.M. Khattab Mater. Res. Technol. 11 (2021) 264.
[35] A.M. Fayad, A.M. Fathi, A.A. El-Beih, M.A. Taha, S.A.M. Abdel-Hameed, Mater. Eng. Perform. 28 (9) (2019) 5661.
[36] M.A. Taha, R.A. Youness, G.T. El-Bassyouni, M.A. Azooz, Silicon (2020).
[37] M.A. Taha, R.A. Youness, M.F. Zawrah, Ceram.Int. 46(15) (2020) 24462.
[38] R.A. Youness, M.A. Taha, H. Elhaes, M. Ibrahim,Mater. Chem. Phy. 190 (2017) 209.
[39] E.B. Moustafa, M.A. Taha, Appl. Phy. A 126(3) (2020)1.
[40] P. Ashwath, J. Joel, M. Anthony Xavior, H.G. Prashantha Kumar, Mater. Today: Proceedings 5(2) (2018) 7329.
[41] S.C. Okumus, S. Aslan, R. Karslioglu, D. Gultekin, H. Akbulut, Mater. Sci. 18(4) (2012). https://dx.doi.org/10.5755/j01.ms.18.4.3093
[42] M.F. Zawrah, H. Abo Mostafa, M.A. Taha, Mater. Res. Express. 6(12) (2019) 125014.
[43] H.S. Kim, Mater. Sci. Eng. A 289 (2000) 30.
[44] H. Abdizadeh, M.A. Baghchesara, Ceram. Int. 39(2) (2013) 2045.
[45] A. Khan, M.W. Abdelrazeq, M.R. Mattli, M.M. Yusuf, A. Alashraf, P.R. Matli, R.A. Shakoor, Crystals 10 (10) (2020) 1.
[46] H. Farajzadeh Dehkordi, M.R. Toroghinejad, K. Raeissi, Mater. Sci. Eng. A 585 (2013) 460.
[47] S.I. Cha, K.T. Kim, S.N. Arshad, C.B. Mo, S.H. Hong, Adv. Mater.17(11) (2005) 1377.
[48] A. Baradeswaran, S.C. Vettivel, A. Elaya Perumal, N. Selvakumar, R. Franklin Issac, Mater. Des. 63 (2014) 620.
[49] C. Velmurugan, R. Subramanian, S. Thirugnanam,, B.A. T. Kannan, JOTSE 2(1) (2011) 49.
[50] M.S. C.S. Ramesh, Wear 263 (2007) 629.